NMR Characterization of Complex *p*-Oligophenyl Scaffolds by Means of Aliasing Techniques to Obtain Resolution-Enhanced Two-Dimensional Spectra

by **Damien Jeannerat***, **Dawn Ronan**, **Yoann Baudry**, **André Pinto**, **Jean-Paul Saulnier**, and **Stefan Matile**

Department of Organic Chemistry, University of Geneva, 30, Quai Ernest Ansermet, CH-1211 Geneva 4

Dedicated to Professor *Ulrich Burger* on the occasion of his 65th birthday

The usefulness of computer-assisted aliasing to secure maximal resolution of signal clusters in ^{1}H- and ^{13}C-NMR spectra (which is essential for structure determination by HMBC 2D NMR spectroscopy) in minimal acquisition time is exemplified by the complete characterization of the two complementary *p*-octiphenyls **1** and **2** with complex substitution patterns. The need for digital resolution near 1 Hz/pt to dissect the extensive signal clusters in the NMR spectra of these refined oligomers excluded structure determination under routine conditions. High resolution was secured by exploiting the low signal density in the ^{13}C dimension of HMBC spectra by using computer-assisted aliasing to maximize signal density. Based on the observed shifts in DEPT and ^{1}H-decoupled ^{13}C-NMR spectra of **1** and **2**, computer-assisted aliasing allowed to reduce the number of required time increments by a factor of 20 to 30 compared to full-width spectra with identical resolution. Without signal-to-noise constraints, this computer-assisted aliasing reduced the acquisition time for high-resolution NMR spectra needed for complete characterization of refined oligomers **1** and **2** by the same factor (*e.g.*, from over a day to about an hour). With resolved signal clusters in fully aliased HSQC and HMBC spectra, unproblematic structure determination of **1** and **2** is demonstrated by unambiguous assignment of all C- and H-atoms. These findings demonstrate that computer-assisted aliasing of the underexploited ^{13}C dimension makes extensive molecular complexity accessible by conventional multidimensional heteronuclear NMR experiments without extraordinary efforts.

Introduction. – Usually, clusters of signals with nearly equivalent chemical shifts are not resolved in 2D NMR spectra. Routine structure determination, however, often requires complete resolution of such signal clusters without extraordinary effort. Because of the quasi-identical repeats in the structures, the NMR spectra of refined oligomers including peptides, oligonucleotides, polysaccharides, polyketides, and terpenoids, these spectra are notoriously difficult to analyze due to signal clustering. A particularly stunning example of signal clustering was encountered upon the completion of the synthesis of refined rigid-rod oligomers **1** and **2** described in the preceding publication [1].

The objective of this report is to exemplify the power of computer-assisted aliasing to resolve signal clusters in liquid-state 2D NMR spectra by the fast, facile, and full assignment of all signals in the ^{1}H- and ^{13}C-NMR spectra of {242}-*p*-octiphenyl **1** and {323}-*p*-octiphenyl **2**. These *p*-oligophenyls are complementary rigid-rod oligomers with refined substitution patterns along their scaffolding (*Fig. 1*). The $1^{3},2^{3},3^{2},4^{3},5^{2},6^{3},7^{2},8^{3}$[1]) motif of {242}-*p*-octiphenyl **1** comprises terminal $1^{3},2^{3}$ and $7^{2},8^{3}$

[1]) Arbitrary numbering; for systematic names, see *Exper. Part* in [1].

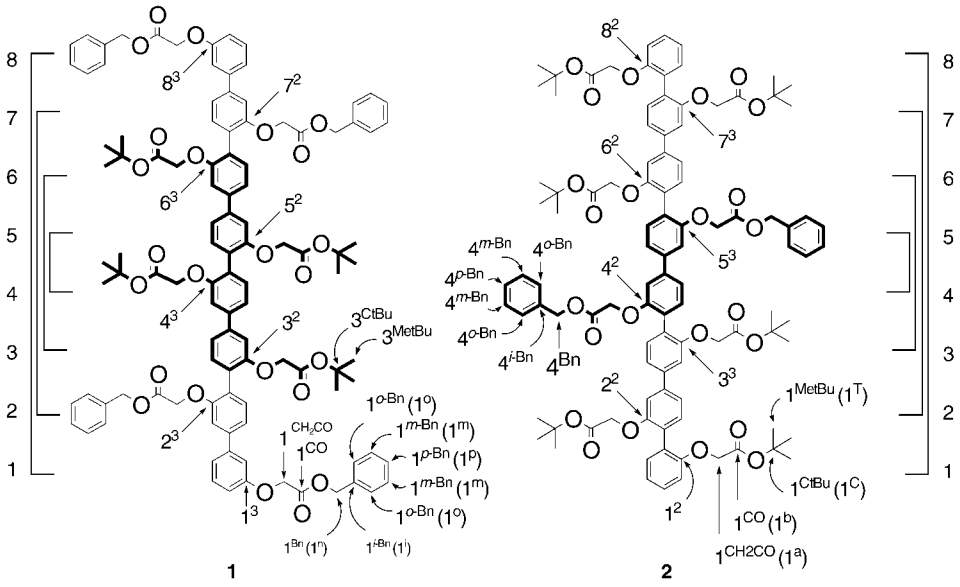

Fig. 1. *Structures of {242}*-p-*octiphenyl* **1** *and {323}*-p-*octiphenyl* **2** *with numbering* (*arbitrary*[1])) *and abbreviations.* The solid lines added on both sides connect identical arenes. The arene–arene torsion angles are not zero, atropisomerism around each arene–arene single bond being possible at room temperature.

domains with substituents that differ only slightly from those of the central 3^2,4^3,5^2,6^3 domain. The complementary 1^2,2^2,3^3,4^2,5^3,6^2,7^3,8^2 [1]) motif of {323}-*p*-octiphenyl **2** contains larger terminal 1^2,2^2,3^3 and 6^2,7^3,8^2 domains that are separated by a compressed central 4^2,5^3 domain with inverted sequence for the same, nearly identical substituents (*i.e.*, central *tert*-butyl esters and terminal benzyl esters in **1**, terminal *tert*-butyl esters and central benzyl esters in **2**). The center of symmetry in the middle of the molecule reduces the number of NMR signals to half the number of atoms (*Fig. 1*, lateral solid lines). The presence of many quasi-symmetrical positions resulted in quite remarkable signal clustering in both the ^{1}H- and ^{13}C-NMR spectra of *p*-octiphenyls **1** and **2** (*Fig. 2*). Highlights included clusters of nearly equivalent C-atoms C(2^3)/C(3^2)/C(4^3) at δ 156, C(2^5)/C(3^6)/C(4^5) at δ *ca.* 132, C(3^5)/C(4^6) at δ 120 ppm, and C(3^b)/C(4^b) at δ 168 in the ^{13}C-NMR spectrum of {242}-rod **1**, and the corresponding C-atoms in the scaffold and side chains of {323}-*p*-octiphenyl **2** (for the trivial locants, see also below, *Fig. 6*).

Today, homonuclear (*e.g.*, ^{1}H,^{1}H COSY) and ^{1}H,^{13}C-heteronuclear (HSQC, HMBC) two-dimensional (2D) NMR spectroscopy is routinely used to assign the signals in one-dimensional ^{1}H- and ^{13}C-NMR spectra. For structure determination of refined oligomers, *e.g.*, **1** and **2**, access to high-resolution 2D NMR spectra is crucial because of signal clustering (*Fig. 2*). Signal separation in the first dimension of 2D spectra requires, however, an increased number of t_1 increments, which results in exceedingly long experimental times [2]. The digital resolution is small when the resolution of the signals is high. For high signal resolution, this imposes a large number of time increments because: digital resolution = spectral width/number of time increments.

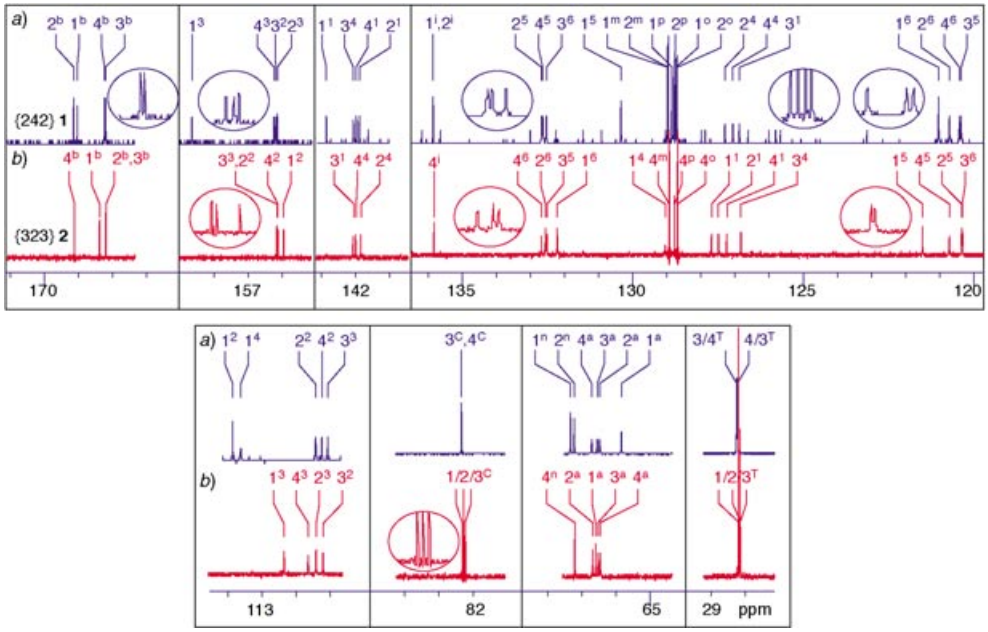

Fig. 2. *Proton-decoupled* ^{13}*C-NMR spectra of* a) *{242}-rod* **1** (blue) *and* b) *{323}-rod* **2** (red) *illustrating signal clusters with peaks often separated by a few Hz only.* The shown assignments were made using aliased HBMC 2D NMR spectroscopy (see below). See *Figs. 1* and *6* for the abbreviations of C-atoms.

This is especially true for high-field spectrometers where the number of time increments needed to resolve signals that are 2 Hz apart may be 100 times above the typical values (*i.e.*, 128 or 256 increments, *Table 1*). With the recent improvements in sensitivity due to higher field strengths, pulse-field gradients, and low-temperature-detection probes, it is more and more common that a satisfactory signal-to-noise ratio is obtained with only a fraction of the number of time increments required for ideal signal

Table 1. *Number of Time Increments of Full-Width*[a]*) 2D Spectra as a Function of Desired Resolution*

Spectrometer frequency [MHz]	Digital resolution [Hz/pt][b])	*TD*[c]) (^{1}H dimension[d])) [pts]	*TD*[c]) (^{13}C dimension[e])) [pts]
400	10[f])	400	2000
400	1[g])	4000	20000
600	10[f])	600	3000
600	1[g])	6000	30000

[a]) For ^{1}H, 10 ppm; for ^{13}C, 200 ppm. [b]) Assuming processing by using zero filling and standard apodization function, a digital resolution of x Hz/pt allows typically to resolve signals more than $2x$ to $4x$ Hz apart. Provided signals are separated in the directly detected dimension, one can resolve signals slightly below x Hz. The limit in digital resolution is given by the spectrometer performance (near 1 Hz) and relaxation properties. Molecules of the size discussed here and smaller allow the maximal t_1 to reach 500 ms, which corresponds to a resolution of 1 Hz/pt. [c]) *TD* = number of time increments required (in points). [d]) For ^{1}H,^{1}H COSY, *etc.* [e]) For ^{1}H,^{13}C HSQC, HMBC, *etc.* [f]) Maximal $t_1 = 50$ ms. [g]) Maximal $t_1 = 500$ ms.

resolution. Due to practical constraints to minimize acquisition time per sample, routine 2D NMR spectra, therefore, have excellent signal-to-noise ratios but poor digital resolution.

In this report, we describe computer-assisted aliasing as a practical method to produce routine 2D NMR spectra with excellent signal-to-noise ratios as well as excellent digital resolution without the need for excessive acquisition time. This method, communicated previously by means of the less-demanding methoxybenzyl analog of {323}-*p*-octiphenyl **2** as an initial example [3] and discussed in detail elsewhere [4–6], is based on a violation of the *Nyquist* condition [2]. In routine 2D NMR spectra, data acquisition covers the full spectral width with all signals. In aliased 2D NMR spectra, data acquisition focuses on a much smaller spectral window [7–9]. In the resulting spectra, signals are 'folded back' or 'aliased' [10] into the smaller spectral window. For example, in the aliased ^{1}H,^{1}H COSY of {242}-*p*-octiphenyl **1**, the cross-peak between H–C(1^4) at δ 6.91 and H–C(1^5) at δ 7.38 (*Fig. 3*,*a*) appeared as cross-peak between the aliased H–C(1^4) – new at δ 7.43 – and H–C(1^5) at the original δ 7.38 (*Fig. 3*,*b*). The positions of 'aliased' signals do not correspond to their chemical shifts. 'Aliasing', exemplified here with H–C(1^4) (*Fig. 3*,*b*), results from a reduction of the spectral width from SW_0 to SW_a in the first dimension of two-dimensional spectra (*Fig. 3*,*c*, left). This causes signals to appear inside the reduced spectral width at a position that depends on the acquisition mode in the t_1 dimension. With the more-common 'States', 'Echo/Antiecho', and 'States-TPPI' methods [10], the resulting aliased spectrum corresponds to an overlay of stripes cut from the conventional spectrum (*Fig. 3*,*c*, bottom center). With the less-common 'TPPI' [10], the resulting 'folded' spectrum looks like the projection through a multiply folded hardcopy of the conventional spectrum (*Fig. 3*,*c*, bottom right). In both cases, the positions of the aliased signals is given by the modulus of the original signal position with respect to the reduced spectral width.

Whereas computer-assisted selection of perfect window boundaries (*i.e.*, spectral width) is unavoidable in heteronuclear experiments like aliased HMBC (below), the situation with homonuclear ^{1}H,^{1}H COSY is less demanding but also less attractive. The spectral diagonal and high signal density increase the probability of overlap between aliased and true cross-peaks in aliased ^{1}H,^{1}H COSY. The reduction of signal surfaces as a function of the square of the field can bypass some of these limitations at high field. However, computer-assisted optimization of homonuclear ^{1}H,^{1}H COSY remains of limited interest because automated spectrum analysis is problematic. Moreover, possible reductions in acquisition time are not as substantial as with heteronuclear ^{1}H,^{13}C experiments like HMBC, and optimization can be done without computer assistance in many cases. Manual aliasing is usually sufficient to exploit occasional silent regions in a ^{1}H-NMR spectrum (*Fig. 3*,*a* and *b*).

In heteronuclear 2D NMR spectroscopy, the ^{13}C dimension exhibits extremely low signal density because ^{1}H-decoupled signals appear as sharp *singlets* distributed over a large spectral width. This low signal density is attractive for computer-assisted aliasing because it leaves much silent space to systematically position aliased or folded signals. Systematic manual elaboration of up to 100-fold reductions in spectral width is, however, not feasible in practice. Computer-assisted determination of optimal aliasing conditions, on the other hand, is unproblematic [5][6]. To do so, a program was created

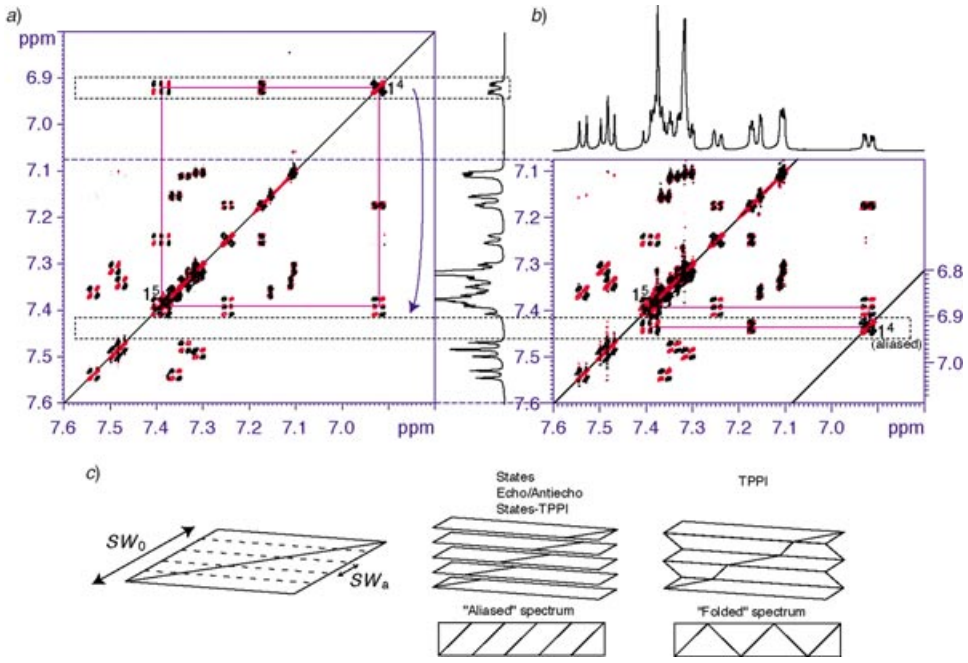

Fig. 3. *Comparison of* a) *conventional and* b) *aliased COSY spectra of {242}-rod* **1** *illustrating aliasing of* $H-C(1^4)$. c) *Methods used to obtain aliased* (left) *or folded high-resolution spectra* (right) *by reducing the spectral width from* SW_0 *to* SW_a *in the first dimension of two-dimensional spectra* (top) [10]. In folded spectra, every other section has inverted scale. See *Fig. 6* for the abbreviations of H-atoms.

that – in response to a list of ^{13}C-NMR chemical shifts – delivers the perfect spectral width for maximal density of real and 'aliased' signals in the ^{13}C dimension [11]. Without signal-to-noise limitations, the reduction of the number of time increments required for complete resolution of signal clusters corresponds directly to the reduction of the spectral width obtained by optimized signal distribution. The number of time increments required after computer-assisted spectral-width optimization can be directly compared with those for a conventional spectrum with identical resolution. To do so, results from computer-assisted aliasing for the measurements of 648 aliased 2D NMR spectra were analyzed (*Fig. 4*). The ratio between time increments required for conventional (–) and fully aliased 2D spectra (···) decreased with increasing molecular mass because of similarly increasing signal density in the ^{13}C-NMR spectra (*Fig. 4*, – – –). The correlation of required time increments and real acquisition time depends on many parameters like desired resolution, analyte concentration (*i.e.*, signal-to-noise ratio), and so on. Nevertheless, assuming 3 seconds per time increment, the total acquisition time for 648 spectra was calculated for full-width and aliasing conditions. This very approximative comparison suggested that computer-assisted aliasing allows the reduction of the acquisition time for 648 spectra of similar quality from almost 6 months for conventional 2D spectra to a little less than 3 days for aliased 2D spectra.

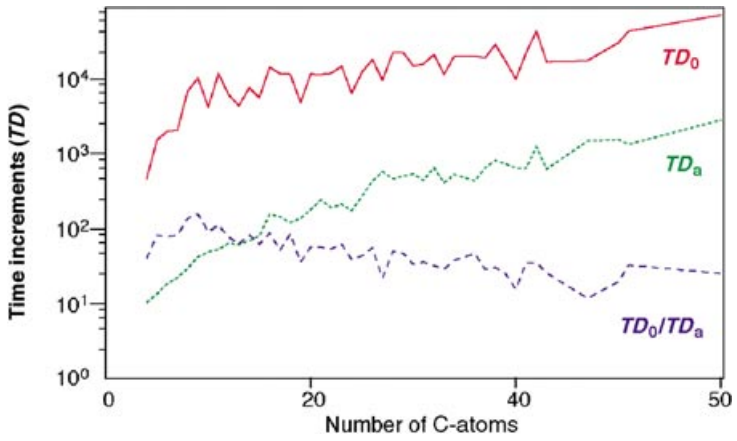

Fig. 4. *Analysis of 648 results from computer-assisted aliasing of a peak lists from DEPT spectra depicted as time increments* (TD_o, TD_a, or TD_o/TD_a) *needed for conventional* (–, TD_o) *and aliased 2D spectra* (···, TD_a) *as well as the time factor of time reduction gained by computer-assisted aliasing* (– – –, TD_o/TD_a) *as a function of C-atoms per molecule*

The efficiency of computer-assisted aliasing increases with increasing spectrometer field strength. At constant spectral width and resolution (1 Hz/pt), the acquisition time for conventional high-resolution spectra increases by 50% when moving from a 400-MHz- to a 600-MHz-^{1}H-*Larmor*-frequency spectrometer because the number of Hz/ppm increases linearly with the magnetic field (*Table 1*). The acquisition time of fully aliased high-resolution spectra, in contrast, increases only slightly with increasing field strength because the number of time increments required for a full separation depends mainly on the number of signals to separate.

Results and Discussion. – The objective of this report was to describe computer-assisted aliasing as a practical method to produce routine 2D NMR spectra with excellent signal-to-noise ratio as well as excellent digital resolution without the need for excessive acquisition time by means of the characterization of refined, complementary {242}-*p*-octiphenyl **1** and {323}-*p*-octiphenyl **2** as pertinent examples (*Fig. 1*). In the ^{1}H-NMR spectra of both oligomers, only aromatic protons display homonuclear couplings. The spectral width in the ^{1}H,^{1}H COSY experiment was therefore focused on this region. This reduction of the spectral width to 0.8 ppm resulted – on a 500-MHz-^{1}H-*Larmor*-frequency spectrometer – in a resolution near 1.5 Hz/pt in 256 increments (*Figs. 3* and *5*).

The ^{1}H,^{1}H COSY spectrum of {242}-*p*-octiphenyl **1** revealed four isolated coupling networks. Identification of the terminal arene 1 was straightforward because coupling occurred between four protons, *i.e.*, H–C(1^2), H–C(1^4), H–C(1^5), and H–C(1^6). Differentiation of the remaining three networks comprising three protons each required resolution of ^4J couplings across the rod axis. To detect these long-range couplings, the choice of pulse sequence was more important than resolution enhancement by computer-assisted aliasing. Phase-sensitive experiments were attractive because the positive and negative signals help to identify the centers of overlapping

long-range cross-peaks (*Fig. 5*, *a*, *b*, *e*, *f*). Alternative sequences with pre-evolution delay [12] to detect small-coupling cross-peaks were not considered because of negligible improvements on resolution. Compared to conventional phase-sensitive COSY, magnitude-gradient COSY or 'gs-COSY' (*Fig. 5*, *c*, *d*) gave better results because the long-range couplings H–C(2^2),H–C(2^6) and H–C(3^3),H–C(3^5) were detectable not only with long (*Fig. 5*, inset *c vs. a* and *e*) but also with short evolution time (*Fig. 5*, inset *d vs. b* and *f*). The absence of phase sensitivity in gs-COSY, however, resulted in an apparent signal broadening that hindered signal differentiation compared to phase-sensitive COSY with the (+/–) signals (*Fig. 5*, inset *c vs. a* and

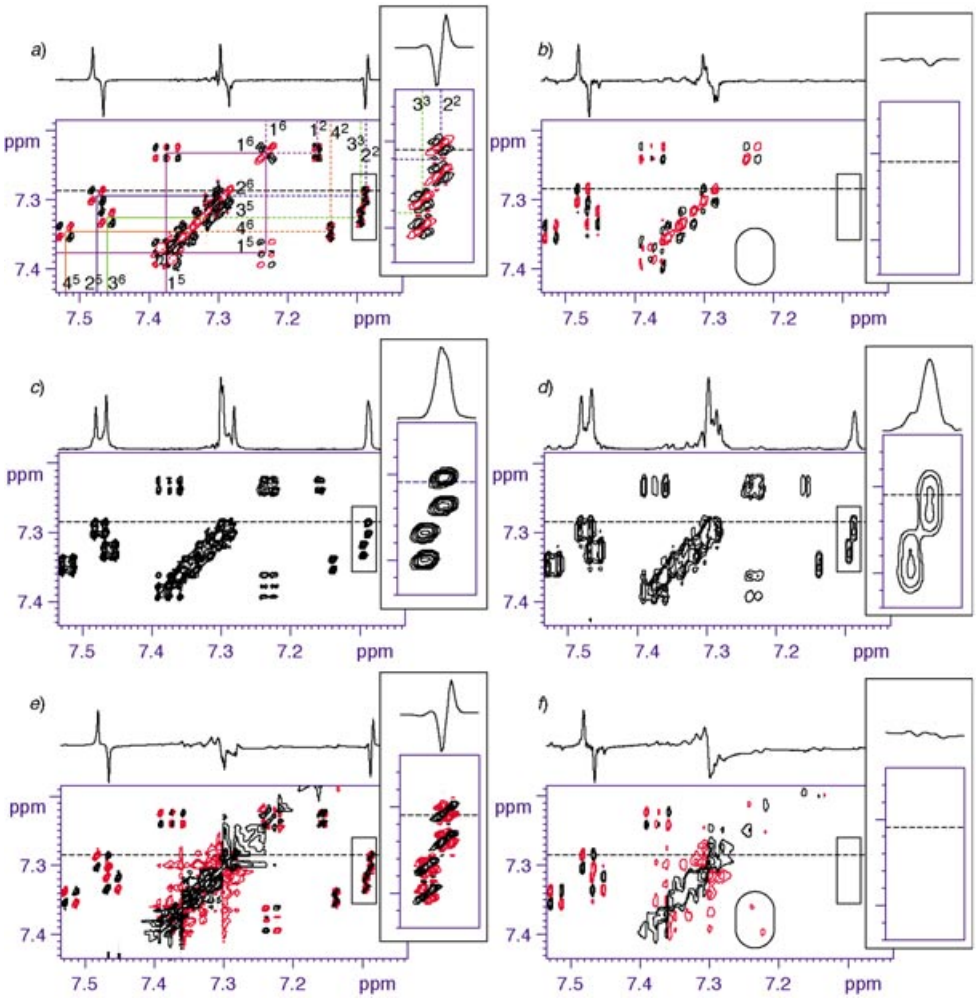

Fig. 5. *Part of* a) b) *phase-sensitive double-quantum-filtered* (DQF), c) d) *magnitude-gradient DQF and* e) f) *conventional phase-sensitive* $^1H,^1H$*-COSY 2D NMR plots of {242}-*p*-octiphenyl* **1** *at high* (a) c) e): 256 × 1024 points in both dimensions) *and low resolution* (b) d) f): 64 × 512 points). The four coupling networks (solid lines –: ^3J; dotted lines ⋯: ^4J) including cross-sections for H–C(2^6) (dashed lines – – –, black) and pertinent clusters (insets) are highlighted. See *Fig. 6* for abbreviations of H-atoms.

e). However, access to cross-peak fine structure provided by phase-sensitive COSY is mainly important for the determination of coupling constants from the COSY experiment [13]. Beginning with the four deshielded protons H–C(1^5), H–C(2^5), H–C(3^6), and H–C(4^5), nearly complete assignment of four discrete coupling networks was straightforward from the COSY spectra of **1** (*Figs. 3*, *5*, and *6*, blue atoms). Assignment of the confirmed coupling networks -2^2-2^5-2^6-, -3^3-3^5-3^6-, and -4^2-4^5-4^6- to arene modules 2, 3, and 4 was, however, not possible without information from computer-assisted aliased high-resolution HMBC.

Application of the lessons learned with the 1^3,2^3,3^2,4^3,5^2,6^3,7^2,8^3 motif of {242}-*p*-octiphenyl **1** to the complementary 1^2,2^2,3^3,4^2,5^3,6^2,7^3,8^2 motif of {323}-*p*-octiphenyl **2** was unproblematic with regard to ^{1}H,^{1}H COSY (*Fig. 7*). Namely, reduction of the spectral width to the pertinent 0.758×0.758 ppm of the aromatic region gave a gradient-enhanced phase-sensitive double-quantum-filtered ^{1}H,^{1}H-COSY 2D-NMR plot with satisfactory resolution of cross-peaks (*Fig. 7,a*). The employed 512 time increments were sufficient to detect ^4J cross-peaks H–C(1^6)/H–C(1^4) and to assign the centers of the overlapping cross-peaks H–C(4^6)/H–C(4^5), H–C(3^6)/H–C(3^5), and H–C(2^6)/H–C(2^5) (*Fig. 7,b*). Consideration of 100 time increments (*Fig. 7,c*) caused disappearance of only long-range cross-peaks because the t_1 evolution is not long enough. Moreover, the resolution of the three main signals was insufficient under these conditions. Assignment of four coupling networks in the COSY plot of **2** was almost as unproblematic as with **1** (*Figs. 7* and *6*, blue atoms). The only remaining ambiguity caused by isochronous H–C(2^5) and H–C(3^6) was eliminated by using information from aliased HBMC (below). The key conclusion that assignment of the coupling networks -2^3-2^5-2^6-, -3^2-3^5-3^6-, and -4^3-4^5-4^6- to arene modules 2, 3, and 4 requires additional information from aliased HMBC was the same as with *p*-octiphenyl **1**.

Most information on the spin networks of {242}-*p*-octiphenyl **1** and {323}-*p*-octiphenyl **2** was secured from long-range correlations in aliased HMBC spectra (*Fig. 6*, arrows). To access this crucial information, identification of some reference protons and C-atoms by COSY and HSQC was, however, important. For **1** and **2**, 13 aromatic protons had been identified in the COSY plot, although assignment of three networks to arenes 2, 3, and 4 remained elusive (*Fig. 6*, blue). The C-atoms attached to these H-atoms were identified by HSQC spectroscopy. Peak assignment was, however, not possible by using conventional HSQC spectra acquired with 256 time increments and 240 ppm spectral width because clustered ^{13}C signals were not resolved (*Fig. 8*). Enlargements of the unoptimized HSQC spectrum of {242}-*p*-octiphenyl **1** revealed that the resolution was nearly two orders of magnitude too low. Excluding less-important side-chain C-atoms, signal clusters comprising C(2^5)/C(3^6)/C(4^5) within 16.9 Hz and C(3^5)/C(4^6) within 6.5 Hz were identified as most problematic.

Even a reduction of the ^{13}C spectral width to the actual width (105 ppm) would require thousands of time increments to achieve a satisfactory resolution (*Table 2*, *Entry 2*). Therefore, computer-assisted determination of the minimal spectral width was unavoidable by using peak lists from either DEPT (for **1**) or ^{1}H-decoupled ^{13}C-NMR spectra (for **2**). The former approach – without quaternary C-atoms – yields perfect acquisition parameters valid for aliased HSQC only, whereas the latter approach yields slightly less-favorable acquisition parameters that are, however, applicable to both aliased HSQC and aliased HMBC spectroscopy. Already without

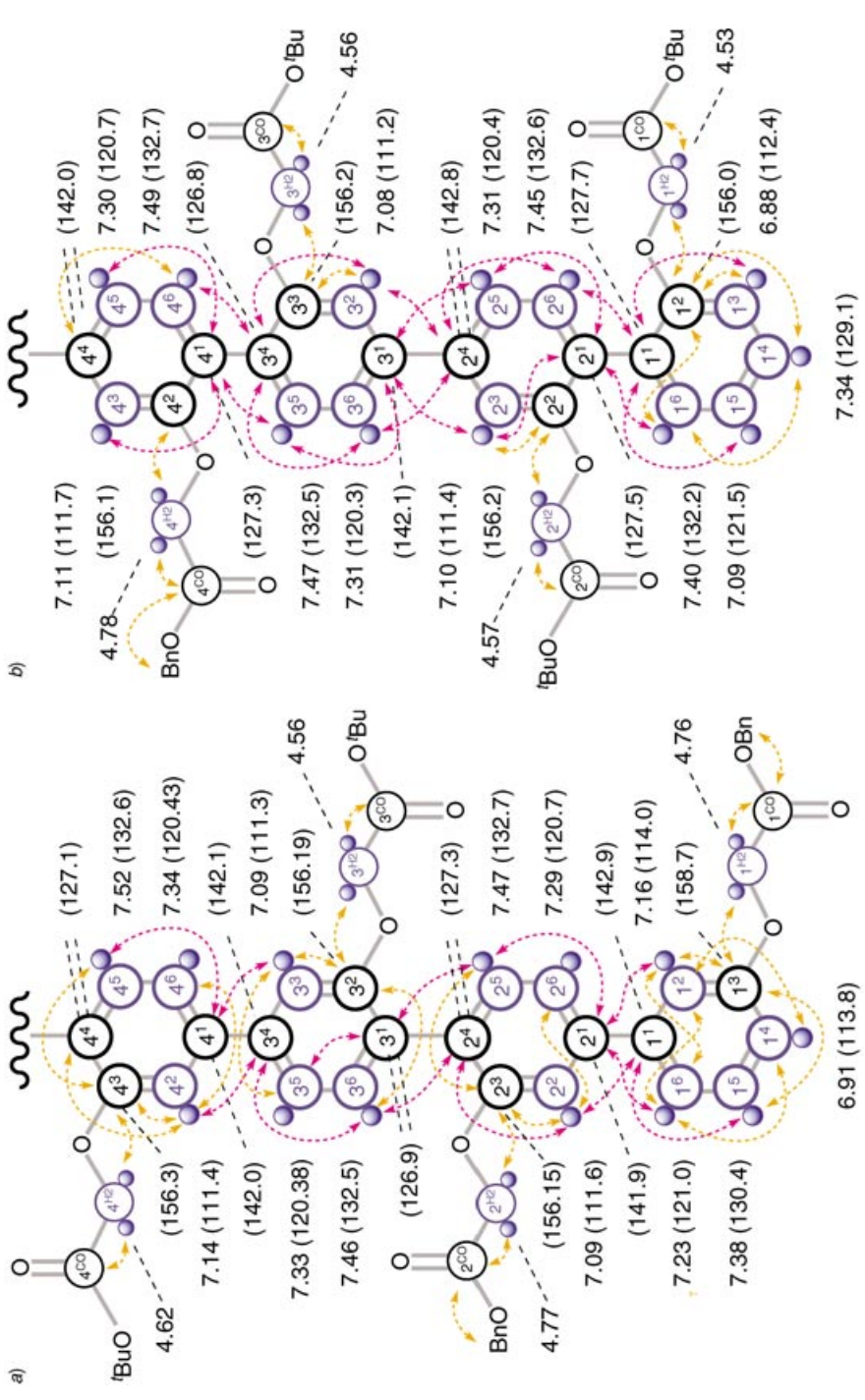

Fig. 6. *Assignment of chemical shifts of* a) *{242}-*p*-octiphenyl* **1** *and* b) *{323}-*p*-octiphenyl* **2** *by aliased HMBC*. Dotted arrows: resolved HMBC signals required to assign, *e.g.*, coupling networks -$2^{2/3}$-2^5-2^6-, -$3^{3/2}$-3^5-3^6-, and -$4^{2/3}$-4^5-4^6- known from ^{1}H,^{1}H COSY and aliased HSQC (blue) to arenes 2, 3, and 4 (magenta). Some of the indicated signals were visible at contour levels different from the ones depicted in *Figs. 11* and *12*.

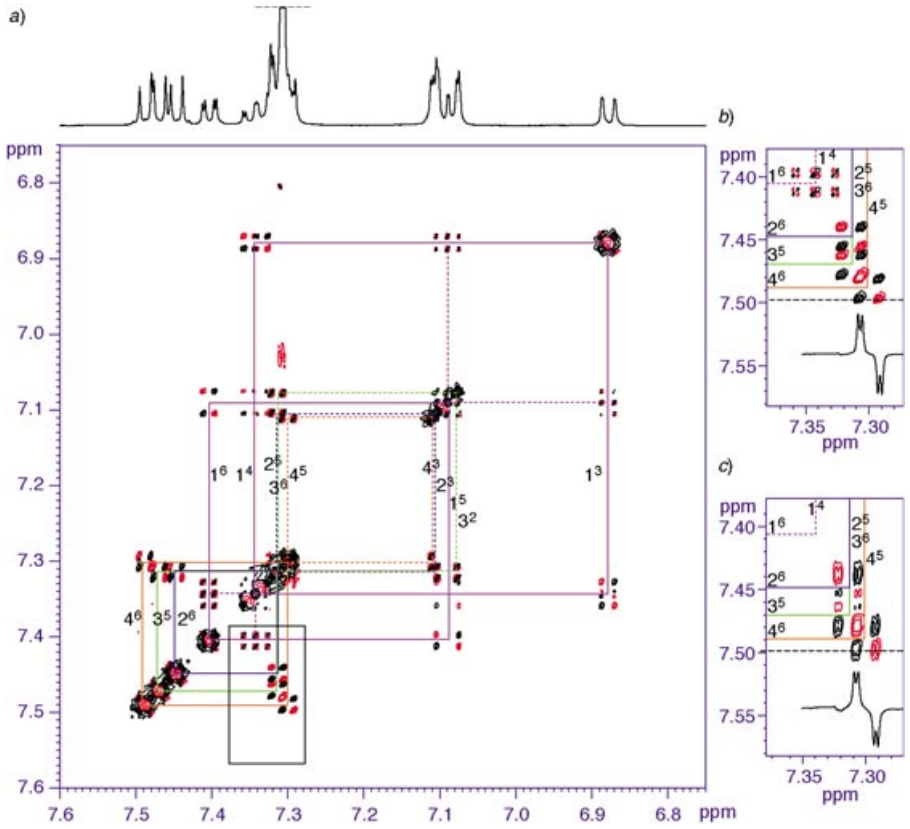

Fig. 7. a) *Gradient-enhanced phase-sensitive double-quantum-filtered* $^{1}H,^{1}H$*-COSY 2D NMR plot of {323}*-p-*octiphenyl* **2** *with assignments* (*cf. Fig. 6*). *Enlargements illustrate* b) *satisfactory* (512 time increments) *and* c) *unsatisfactory resolution* (100 time increments) *with cross-sections of* $H-C(4^{6})/H-C(4^{5})$ (dotted lines). See *Fig. 6* for abbreviations of H-atoms.

consideration of the here less-influential proton dispersion [4], reduction factors of 25.3 and 22.6 were obtained for **1** (*via* DEPT) and **2** (*via* ^{1}H-decoupled ^{13}C-NMR), respectively. Because of an unproblematic signal-to-noise ratio, these reduction factors corresponded directly to the reduction of acquisition times. Therefore, in the present case, computer-assisted aliasing provided spectra in 90 min with a quality that would require more than 30 h of acquisition under unoptimized conditions.

Allowing for overlap of signals with different ^{1}H dispersion, as can be appreciated from overlap of C(2^{m}) with C(1^{n}) and C(1^{p}) with C(2^{n}) [5], computer-assisted aliasing considering the DEPT data provided an optimal spectral width of 516.61 Hz (*i.e.*, 4.13 ppm) in the ^{13}C dimension. To secure unambiguous H–C correlation of resolved ^{13}C clusters, the resolution in the ^{1}H dimension had to be similar to that required in the ^{13}C dimension. Within meaningful acquisition time, an aliased HSQC spectrum of {242}-*p*-octiphenyl **1** with completely resolved signal clusters was obtained (*Fig. 9*,*a*). In the ^{13}C dimension, the conventional ppm scale was replaced by a frequency-encoded

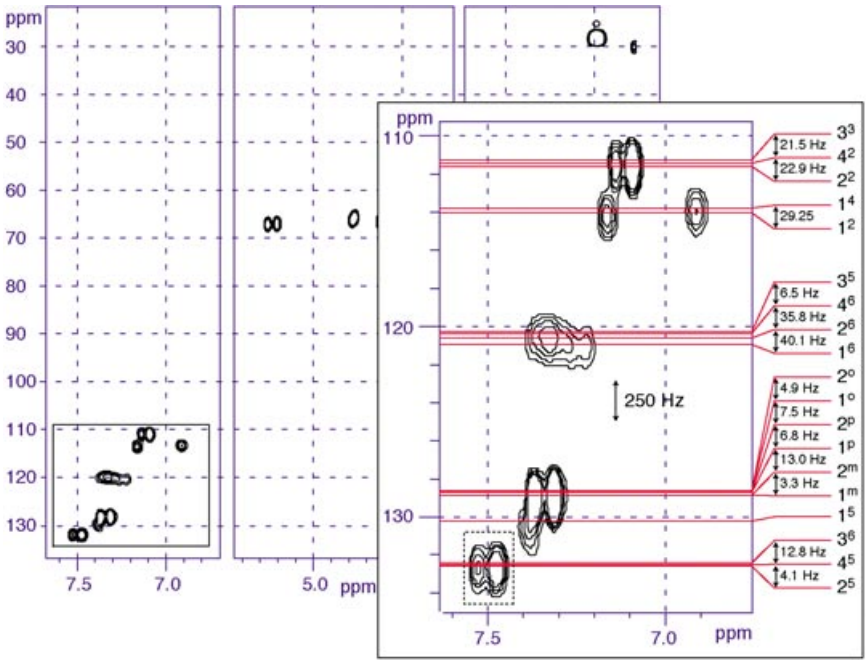

Fig. 8. *Unoptimized HSQC spectrum of {242}-*p*-octiphenyl* **1** (240 ppm spectral width, ^{13}C dimension). Insets highlight unresolved signal clusters (*cf. Fig. 9*). See *Figs. 1* and *6* for abbreviations of C-atoms.

Table 2. *Time-Increment and Spectral-Width Requirements for* **1** *and* **2** *at 500-^1H-*Larmor *Frequency*

Entry	Compd.	Experiment	*TD* [pts][a])	Acquisition time [h]	*ns*/*TD*[b])	*SW* [Hz][c])	Relative *SW*[c])
1	**1**	HSQC[d])	29500	87.1	2[l])	30000.00	58.1
2	**1**	HSQC[e])	12838	38.0	2[l])	13055.75	25.3
3	**1**	HSQC[f])	508	1.5	2[l])	516.61	1.0
4	**2**	HSQC[d])	26562	77.8	2[l])	30000.00	51.8
5	**2**	HSQC[g])	11568	33.9	2[l])	13065.25	22.6
6	**2**	HSQC[h])	512	1.4	2[l])	578.25	1.0
7	**1**	HMBC[i])	36270	53.8	2	35000.00	53.8
8	**1**	HMBC[j])	18254	27.1	2	17614.50	27.1
9	**1**	HMBC[h])	674	16.2	32[m])	650.41	1.0
10	**2**	HMBC[i])	30990	24.8	2	35000.00	60.5
11	**2**	HMBC[k])	15602	12.5	2	17620.13	30.5
12	**2**	HMBC[h])	512	13.1	32[m])	578.25	1.0

[a]) *TD* = number of time increments required (in points). [b]) *ns*/*TD* = number of scans (*ns*) per time increment (*TD*). [c]) *SW* = spectral width, ^{13}C dimension. [d]) Assuming *SW* = 240 ppm. [e]) Assuming SW_0 = 104.446 ppm (from DEPT). [f]) Result from computer-assisted aliasing (from DEPT and HSQC[d])). [g]) Assuming SW_0 = 104.522 ppm (from DEPT). [h]) Result from computer-assisted aliasing (from ^1H-decoupled ^{13}C-NMR spectrum). [i]) Assuming *SW* = 280 ppm. [j]) Assuming SW_0 = 140.916 ppm (from ^1H-decoupled ^{13}C-NMR spectrum). [k]) Assuming SW_0 = 140.961 ppm (from ^1H-decoupled ^{13}C-NMR spectrum). [l]) Used to eliminate experimental artifacts observed with *ns* = 1. [m]) With normal HMBC sequence; alternative t_1-gradient-coding-free sequence (*Fig. 13*) requires only four scans per increment for a satisfactory signal-to-noise ratio.

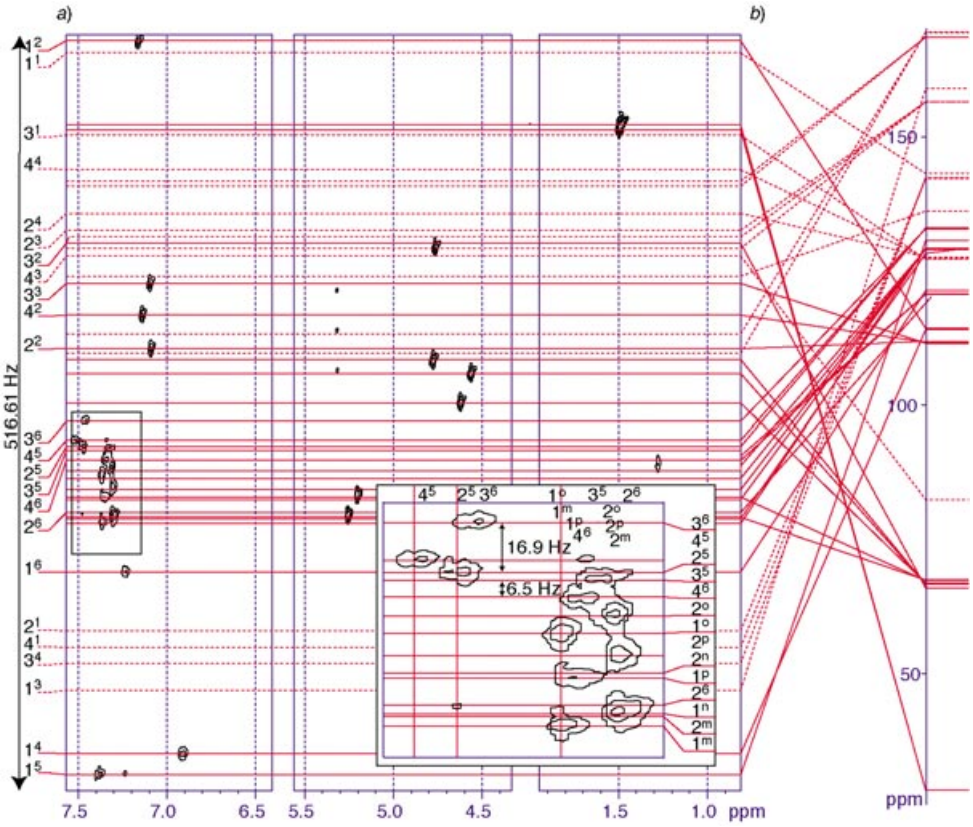

Fig. 9. a) *Aliased HSQC spectrum of {242}*-p-*octiphenyl* **1** (4.13 ppm spectral width, ^{13}C dimension) *with* b) *automated conversion to the schematic ppm scale and insets highlighting resolution of otherwise problematic signal clusters* (*cf. Fig. 8*). See *Figs. 1* and *6* for abbreviations of atoms.

axis. Computer-assisted aliasing provided a list of signal positions in the aliased spectrum to decode these graphics and unfolded automatically the aliased spectrum into a schematic 1D format with the familiar chemical shifts in ppm (*Fig. 9*, *b*).

In the aliased HSQC spectrum of {242}-rod **1**, all ^{13}C clusters of the *p*-octiphenyl scaffold were resolved. The most-problematic signal clusters identified in conventional HSQC (*Fig. 8*, inset) like C(2^5)/C(3^6)/C(4^5) within 16.9 Hz or C(3^5)/C(4^6) within 6.5 Hz appeared as clearly separated signals (*Fig. 9*, inset). With the aliased HSQC, all C–H groups could be correlated to coupling networks identified in the $^1H,^1H$ COSY. Although assignment to specific arene modules 2, 3, and 4 was possible with neither HSQC nor with $^1H,^1H$ COSY, identification of these C–H coupling networks was important to facilitate complete characterization by computer-assisted aliased high-resolution HMBC.

Application of computer-assisted aliasing as described above to {323}-*p*-octiphenyl **2** corroborated the above findings without exception (*Fig. 10*). In the obtained aliased HSQC spectrum, all signals required for structure determination were resolved

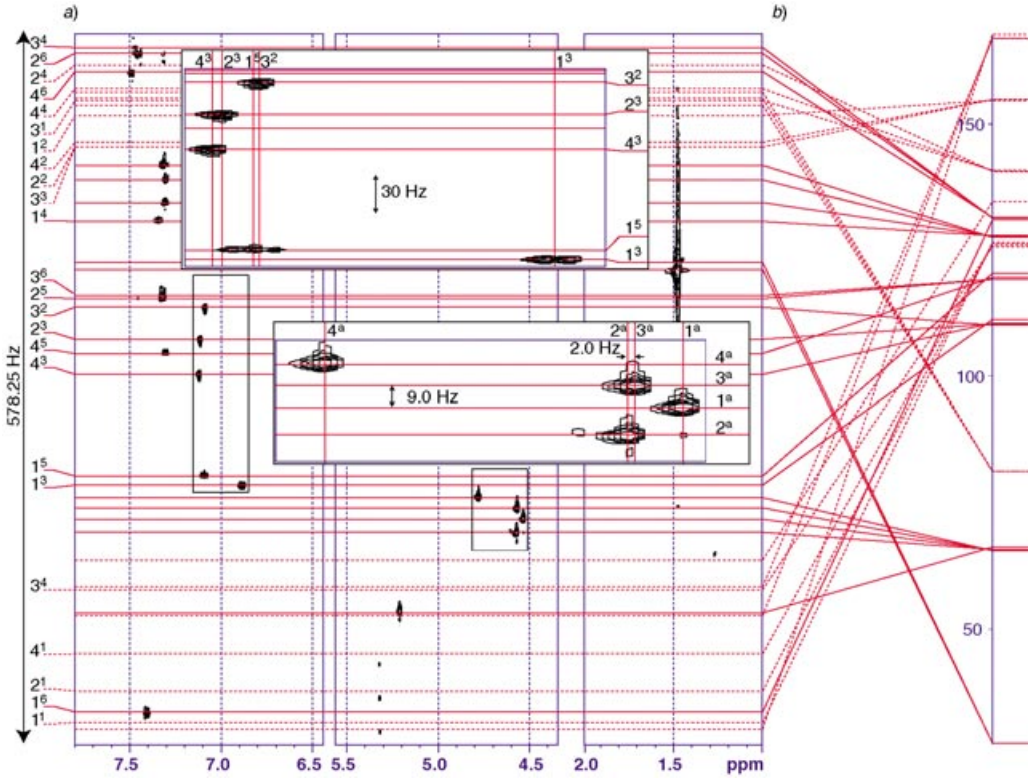

Fig. 10. a) *Aliased HSQC spectrum of {323}*-p-*octiphenyl* **2** (4.6 ppm spectral width, ^{13}C dimension) *with* b) *automated conversion into schematic ppm scale and insets highlighting resolution of problematic signal clusters*. See *Figs. 1* and *6* for abbreviations of atoms.

including one-bond correlations of the quasi-identical H–C(1^3), H–C(1^5), H–C(2^3), H–C(3^2), and H–C(4^3) in the scaffold (inset top) and H–C(1^a), H–C(2^a), H–C(3^a), and H–C(4^a) in the side chains (inset, bottom). The signals for H–C(2^3) and H–C(4^3) near 7.1 ppm or H–C(2^a) and H–C(3^a) near 4.6 ppm illustrated that resolution in the ^1H dimension similar to that achieved in the aliased ^{13}C dimension is important to secure unambiguous H–C correlations.

Computer-assisted aliasing was used as described above to maximize the resolution of the HMBC spectrum of {242}-*p*-octiphenyl **1** (*Fig. 11*). All signals appeared as *m* structures because of scalar coupling. Location of the center of each *m* for unambiguous assignment of ^{13}C signals was unproblematic with the achieved resolution. Notorious signal clusters H–C(2^5)/H–C(3^6)/H–C(4^5) (*Fig. 5*) but also ^{13}C clusters unique for HBMC and essential for structure determination like C(2^1)/C(3^4)/C(4^1) at 142 ppm within 21.9 Hz or C(2^3)/C(3^2)/C(4^3) at 156 ppm within 12.5 Hz could be identified (*Fig. 11*, inset).

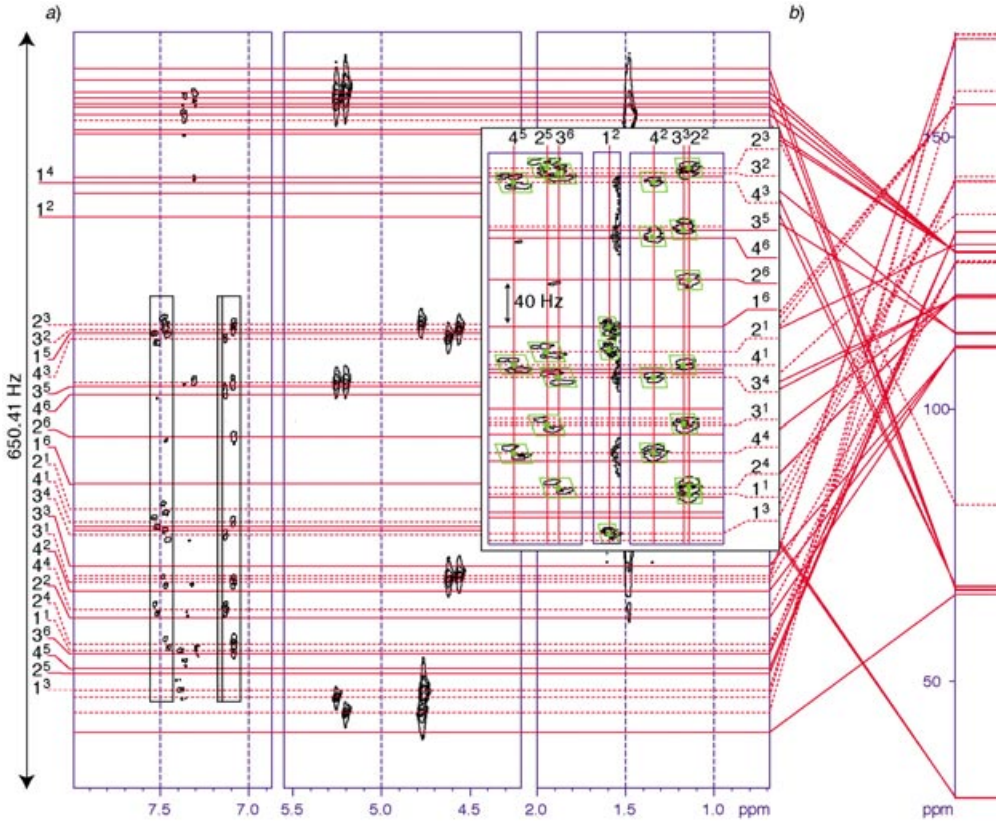

Fig. 11. a) *Aliased HMBC spectrum of {242}*-p-*octiphenyl* **1** (650.41 Hz = 5.20 ppm spectral width, ^{13}C dimension) *with* b) *automated conversion into schematic ppm scale and insets highlighting resolution of signal clusters pertinent for the assignment of interaromatic correlations.* Contour levels are different in each subregion, and quaternary C-atoms are identified by dotted lines. See *Fig. 6* for abbreviations of atoms.

Because of the achieved digital resolution near 1 Hz, assignment of the confirmed proton-coupling networks (*Fig. 6*, blue atoms) to arene modules 2, 3, and 4 was possible (*Fig. 6*, arrows, magenta). Specifically, the connection of arene 2 to the assigned terminal arene 1 was demonstrated by the cross-peak sequence $H-(1^2)/C(2^1)/H-C(2^5)$ (*Fig. 6* and *11*, magenta). This assignment was corroborated by the sequences $H-C(1^5)/C(1^1)/H-C(2^2)$ and $H-C(1^6)/C(2^1)/H-C(2^5)$. This overassignment was important to exclude overinterpretation of resolved yet complex signal clusters. For example, the signal $C(2^3)/H-C(2^5)$ is near $C(3^2)/H-C(3^6)$ or the signal $C(1^1)/H-C(2^2)$ overlaps partially with $C(2^4)/H-C(2^2)$ and could also be misassigned as $C(1^1)/H-C(3^3)$ (*Fig. 11*, inset). The connection between arene 2 and arene 3 was established by the cross-peak sequence $H-C(2^2)/C(2^4)/H-C(3^6)$ (*Fig. 6* and *11*, magenta) and corroborated with sequences $H-C(2^5)/C(3^1)/H-C(3^3)$ and $H-(2^5)/C(3^1)/H-C(3^5)$. Arene 4 was connected to the assigned arene 3 by the cross-peak sequence $H-C(3^6)/C(3^4)/H-C(4^2)$ and corroborated by $H-C(3^3)/C(4^1)/H-C(4^5)$.

Identification of the side chains was unproblematic by using signals of the assigned atoms C(1^3), C(2^3), C(3^2), and C(4^3) to the corresponding CH_2 H-atoms and, from there, to the C=O atoms C(1^b), C(2^b), C(3^b), and C(4^b). The cross-peaks from C(1^b) and C(2^b) only to the benzylic H-atoms and from there to the C_{ipso} and C_o atoms of the benzyl groups confirmed that the benzyl ester side chains are attached to arenes 1 and 2 but not to arenes 3 and 4. Although less relevant for structure determination of {242}-*p*-octiphenyl **1**, full assignment of these lateral arenes was also feasible [14] because of absent cross-peaks in the COSY between 7.36 ppm (benzyl 1) and 7.30 ppm (benzyl 2) (not shown).

Application of the lessons learned from {242}-*p*-octiphenyl **1** to resolve the HMBC spectrum of {323}-*p*-octiphenyl **2** was unproblematic (*Fig. 12*). The key to high-resolution was systematic minimization of the spectral width to 4.6 ppm by computer-assisted aliasing [11]. With the achieved digital resolution near 1 Hz, the crucial assignment of confirmed proton-coupling networks to arene modules 2, 3, and 4 was possible (*Fig. 6*, arrows, magenta). For example, the nearly identical C(2^2) and C(3^3)

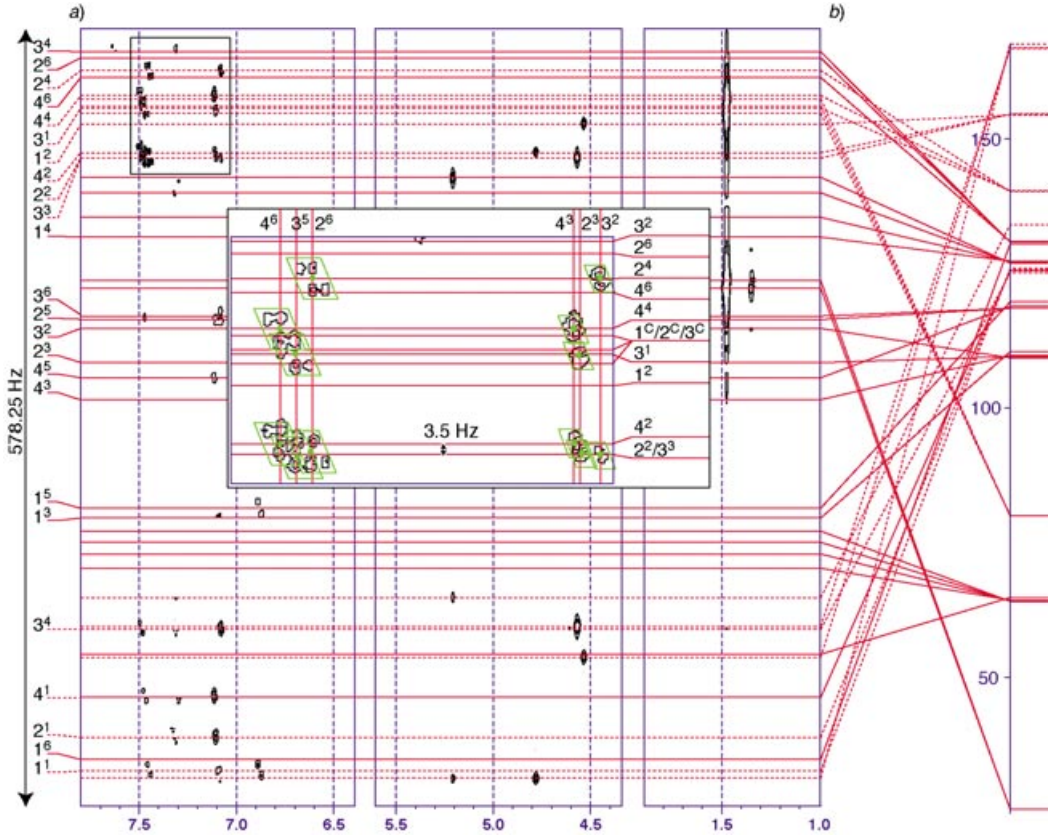

Fig. 12. a) *Aliased HMBC spectrum of {323}*-p-octiphenyl **2** (578.25 Hz = 4.60 ppm spectral width, ^{13}C dimension) *with* b) *automated conversion into schematic ppm scale and insets highlighting resolution of pertinent signal clusters.* Contour levels are different in each subregion. See *Figs. 1* and *6* for abbreviations of atoms.

were distinguishable from the signals C(2^2)/H−C(2^6) and C(3^3)/H−C(3^5), respectively (*Fig. 12*, inset). Proceeding as with rod **1**, overdetermination of critical connectivities between arene modules in the rigid-rod scaffold of **2** was again essential to exclude eventual misinterpretation of resolved but complex signal clusters. This was possible with cross-peak sequences H−C(1^3)/C(1^1)/H−C(2^6) and H−C(1^6)/C(2^1)/H−C(2^3) to connect arenes 1 and 2, sequences H−C(2^6)/C(2^4)/H−C(3^2) and H−C(2^3)/C(3^1)/H−C(3^5) to connect arenes 2 and 3, and sequences H−C(3^2)/C(3^4)/H−C(4^6) and H−C(3^5)/C(4^1)/H−C(4^3) to connect arenes 3 and 4.

We thank the University of Geneva and the *Swiss National Science Foundation* for financial support (200020-101486 and *National Research Program* Supramolecular Functional Materials 4047-057496).

Experimental Part

General. ^{1}H- and ^{13}C-NMR Spectra: *Bruker-DRX* 500-MHz-^{1}H-*Larmor*-frequency spectrometer at 303 K; chemical shifts δ in ppm relative to $SiMe_4$ (= 0 ppm). In aliased 2D HSQC/HMBC spectra, the ^{13}C dimension is depicted in Hz with conversion into δ (in ppm) relative to $SiMe_4$ (= 0 ppm). {242}-*p*-Octiphenyl **1** and {323}-*p*-octiphenyl **2** were synthesized and characterized as described in [1]. A comprehensive list of all peaks in their ^{1}H- and ^{13}C-NMR spectra has been reported previously [1][3].

Computer-Assisted Aliasing. The list of chemical shifts from the ^{1}H-decoupled ^{13}C-NMR spectrum of **1** was submitted to the internet-based program [11] to determine optimal spectral width and number of time increments for aliased HMBC. For the aliased HSQC, a modified version including dispersion in the ^{1}H dimension in a normal HSQC spectrum was used [5]. For **2**, the list of chemical shifts from ^{1}H-decoupled ^{13}C-NMR spectra for both aliased HMBC and the aliased HSQC was applied by using the internet-based program. The carrier frequency of the two-dimensional HSQC/HMBC experiment data set, the scale shift correction of the one-dimensional ^{13}C-NMR spectrum and the spectrometer frequency were also posted on the internet form to simplify scaling of the aliased spectra. For **1**, application of computer-assisted aliasing gave an optimal pair of ^{13}C spectral width $SW_a = 516.61$ and number of time increment $TD_a = 508$ for aliased HSQC, and $SW_a = 650.41$ and $TD_a = 674$ for aliased HMBC. For **2**, $SW_a = 578.25$ and $TD_a = 512$ were used for both aliased HSQC and aliased HMBC. The other acquisition parameters are listed in *Table 3*. The quadrature detection in the ^{13}C dimension was 'echo-antiecho', whereas 'TPPI' acquisition was not applicable (see *Fig. 3*). Graphics

Table 3. *Acquisition Parameters of 2D NMR Spectra of* p-*Octiphenyls* **1** and **2**

	1					**2**					
	Dim[a])	COSY	Full-width HSQC	Optimized HSQC	Optimized HMBC	Dim[a])	COSY	Optimized HSQC	Optimized HMBC	Optimized HMBC[b])	Optimized HMBC[c])
Figure		*3, 5*	*8*	*9*	*11*		*7*	*10*	*12*	*13*	*13*
TD [pts][d])	t_1	256	256	508	674	t_1	512	512[e])	512[e])	776	776
SW [Hz][f])	t_1	379.25	117.91	516.61	650.41	t_1	379.56	578.25	578.25	586.29	586.29
t_1 max	t_1	0.338	1.086	0.492	0.518	t_1	0.649	0.443	0.443	0.487	0.487
Hz/pt	t_1	1.481	0.461	1.017	0.965	t_1	0.771	1.129	1.129	1.026	1.026
TD [pts][d])	t_2	1024	1024	4096	4096	t_2	248	4096	4096	4096	4096
SW [Hz][f])	t_2	379.25	480.82	4280.8	4280.8	t_2	394.57	4844.96	4844.96	4496.40	4496.40
Acq. time [s]		1.350	1.065	0.478	0.479		2.595	0.423	0.423	0.455	0.455
Scan/increment		8	4	4	32		2	2	64	4	4
Total acq. time [min]		80	35	92	970		67	83	787	131	132

[a]) Dim = dimension. [b]) Normal HMBC sequence. [c]) t_1-Gradient-coding-free HMBC sequence. [d]) *TD* = number of time increments (in points). [e]) That the number of optimized increments is a power of 2 is accidental. [f]) *SW* = spectral width.

including conversion of the expanded ^{13}C dimension in Hz into the conventional ppm scale (*Figs. 9–12*) were obtained automatically with the stand-alone version of the program (available on request from the corresponding author).

COSY. Acquisition parameters of COSY are given in *Table 3*. All the sequences used the standard *Bruker* pulse program. Processing of the high-resolution spectra was made with all the acquisition points, the low resolution used the first 64 and 512 points in the first and second dimensions, respectively.

HSQC and HMBC. All reported spectra were obtained with standard HSQC [15–18] and HBMC [19–21] sequences. Better results could be obtained with a modification to the HMBC sequence (*Fig. 13*). This sequence avoids the decrease of signal caused by molecular diffusion during the second half of the t_1 evolution time of the standard sequence [22]. This problem is not specific to computer-assisted aliasing described in this report but it is more likely to cause problems in aliased spectra because high-resolution increases t_1. Instead of a total experimental time of 13–16 h with standard methods, these times could be reduced to a couple of hours, by using the modified sequence. All other acquisition parameters are shown in *Table 3*. To benefit from increased resolution in the ^1H dimension, the number of acquisition points should reside between ½ and 1 s. This insures that the processed spectra have resolution close to the limit of the spectrometer performances. Would sample quantity be an issue or relaxation unfavorable for such a long acquisition, one could acquire data for a long acquisition time and later decide to disregard the last part of the FID when running the *Fourier* transform. This allows to process data differently for regions where resolution is a problem and where signal-to-noise ratio is critical. One can estimate the impact of such a reduction on the line-width in the ^1H dimension knowing that it equals approximately half of the inverse of the effective sampling time. Spectra were processed by using standard parameters. Just like normal 2D experiments, aliased spectra needed no phasing in the first dimension.

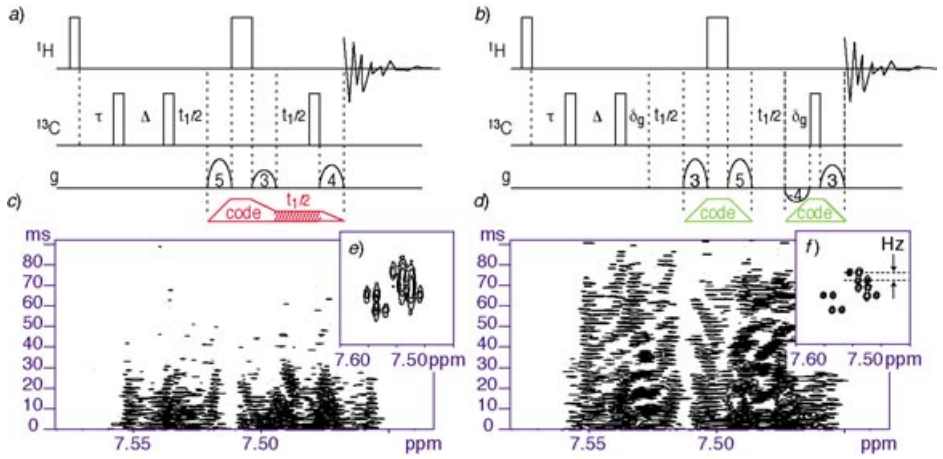

Fig. 13. *Comparison of* a) *normal and* b) t_1*-gradient-coding-free HMBC sequences.* The second sequence completely separates the gradient-selection elements in two parts to avoid the long second half of the t_1 evolution to take place during a gradient-coded period. The phase cycling is unchanged when compared to the standard sequence. In its minimal form, the receiver and the second pulse have 0/180 cycling, while all other pulses remain at 0. With maximal t_1 of 487 ms, the decay of the magnetization is three times slower in *d*) than *c*). This results in improved resolution after *Fourier* transformation *e*) *vs. f*). Both spectra were recorded with 766 time increments with $NS = 4$ and required 2 h of acquisition. With three times less signals and equivalent noise, t_1-gradient-coding-free HMBC requires nine times fewer scans than normal HMBC to reach the same signal-to-noise ratio and signal resolution.

REFERENCES

[1] Y. Baudry, D. Ronan, D. Jeannerat, S. Matile, *Helv. Chim. Acta* **2004**, *87*, 2181.
[2] T. D. W. Claridge, in ' High Resolution NMR Techniques in Organic Chemistry', Vol. 19, Ed. J. E. Baldwin, Pergamon, Oxford, 1999, p. 52.
[3] D. Ronan, Y. Baudry, D. Jeannerat, S. Matile, *Org. Lett.* **2004**, *6*, 885.
[4] D. Jeannerat, *Magn. Reson. Chem.* **2000**, *38*, 415.
[5] D. Jeannerat, *Magn. Reson. Chem.* **2003**, *41*, 3.
[6] D. Jeannerat, in preparation.
[7] R. C. Morshauser, E. R. P. Zuiderweg, *J. Magn. Reson.* **1999**, *77*, 232.
[8] U. Eggenberger, P. Pfaendler, G. Bodenhausen, *J. Magn. Reson.* **1988**, *77*, 192.
[9] K. D. Bishop, P. N. Borer, I. Pelczer, *J. Magn. Reson.*, *Ser. B* **1996**, *110*, 9.
[10] J. Cavanagh, W. J. Fairbrother, A. G. Palmer III, N. J. Skelton, 'Protein NMR Spectroscopy. Principles and Practice', Academic Press, San Diego, 1996.
[11] http://rmn.unige.ch/simplealias.
[12] A. Bax, *J. Magn. Reson.* **1981**, *44*, 542.
[13] D. Jeannerat, *Magn. Reson. Chem.* **2000**, *38*, 156.
[14] E. Pretsch, 'Tables of Spectral Data for Structure Determination of Organic Compounds', Springer Verlag, Berlin, 1989.
[15] L. E. Kay, P. Keifer, T. Saarinen, *J. Am. Chem. Soc.* **1992**, *114*, 10663.
[16] A. G. Palmer III, J. Cavanagh, P. E. Wright, M. Rance, *J. Magn. Reson.* **1991**, *93*, 151.
[17] G. Kontaxis, J. Stonehouse, E. D. Laue, J. Keeler, *J. Magn. Reson.*, *Ser. A* **1994**, *111*, 70.
[18] J. Schleucher, M. Schwendinger, M. Sattler, P. Schmidt, O. Schedletzky, S. J. Glaser, O. W. Sorensen, C. Griesinger, *J. Biomol. NMR* **1994**, *4*, 301.
[19] A. Bax, M. F. Summers, *J. Am. Chem. Soc.* **1986**, *108*, 2093.
[20] G. E. Martin, *Ann. Rep. NMR Spectrosc.* **2002**, *46*, 37.
[21] W. Willker, D. Leibfritz, R. Kerssebaum, W. Bermel, *Magn. Reson. Chem.* **1993**, *31*, 287.
[22] J. Ruiz-Cabello, G. W. Vuister, C. T. W. Moonen, P. van Gelderen, J. S. Cohen, P. C. M. van Zijl, *J. Magn. Reson.* **1992**, *100*, 282.

Received April 27, 2004